

Spin-current Kondo effect: Kondo effect in the presence of spin accumulation

Damian Tomaszewski ¹, Piotr Busz ^{1,2} and Jan Martinek ¹

¹*Institute of Molecular Physics, Polish Academy of Science, Smoluchowskiego 17, 60-179 Poznan, Poland*

²*Institute of Spintronics and Quantum Information, Faculty of Physics, Adam Mickiewicz University, Uniwersytetu Poznańskiego 2, 61-614 Poznan, Poland*

 (Received 20 April 2021; revised 12 July 2021; accepted 16 August 2021; published 7 September 2021)

We present a detailed theoretical description of the influence of the spin accumulation in metallic Fermi leads on the Kondo effect in systems such as quantum dots and Kondo alloys. We discuss an interplay of the spin accumulation, magnetic field, and ferromagnetic leads spin polarization on the Kondo spin-dependent densities of states, conductance, and resistance. It has been shown that the presence of the above-mentioned factors by breaking the spin symmetry leads to the suppression of the Kondo effect. However, for appropriately selected parameter values, these effects can compensate each other, which may lead to the restoration of the Kondo effect in the analyzed systems. We also address some recent experiments related to the spin current in the Kondo alloys.

DOI: [10.1103/PhysRevB.104.125108](https://doi.org/10.1103/PhysRevB.104.125108)

I. INTRODUCTION

The Kondo effect is related to a screening of the quantum dot (or impurity) spin by nearby free electrons, therefore it takes place when the dot is magnetic. Below a certain characteristic temperature T_K , called the Kondo temperature, the unpaired electron in the quantum dot hybridizes with the conduction band states in the leads, which generates a Kondo resonance [1–4].

In the view of spintronics the important issue is the Kondo screening in the presence of spin effects due to, e.g., magnetic field, ferromagnetic leads, or nonequilibrium spin accumulation. In this paper we focus on the spin accumulated nano-systems. The nonequilibrium spin accumulation can be defined as the energy difference between electrochemical potentials of electrons with the opposite spin directions in a given conducting material that is induced by the presence of the nonequilibrium spin current. The spin accumulation can be realized experimentally by spin injection to Kondo alloys [5] or electrodes of the quantum dot system [6]. The best system allowing for studying of the spin accumulation is nonlocal lateral spin valve (LSV) [7–14], where the spin current J is separated from the charge current I . Use of LSV geometry allows for isolation from other spin-related phenomena, such as spin-dependent interface scattering, anisotropic magnetoresistance, and Hall effects. The influence of spin accumulation on the Kondo effect has also been the subject of theoretical research in the systems of nonmagnetic conductor containing magnetic impurities [15], a quantum dot (QD) coupled to a normal and ferromagnetic lead [16], a QD coupled to one normal and one spin accumulated lead [17], and a QD coupled to a normal and superconducting lead [18]. In this work we present the extension of these research by exploring the interplay of various spin effects. Our main focus will not be the way the spin accumulation is generated (that can be found in Refs. [5–14]) but rather the theoretical analysis of its

influence on the behavior of densities of states on the quantum dot (QD) in the Kondo regime, coupled to leads in which spin accumulation occurs. In this way spin accumulation modifies the conductance signal of the dot in relation to the spin-dependent electrochemical potentials in the leads. The spin accumulation is found out to be another method of modifying the behavior of systems with the QD coupled to conductors apart from the ferromagnetic lead polarization [19–36] and magnetic field [37–41] effects. Next, we discuss the interplay of the spin accumulation, magnetic field, and ferromagnetic leads spin polarization on the Kondo spin-dependent densities of states, conductance, and resistance. In the presence of the above-mentioned factors, breaking the spin symmetry leads to the suppression of the Kondo effect. However, appropriate tuning of the system parameters can lead to the restoration of the Kondo effect in the analyzed systems, by mutual compensation of the discussed effects. We will also show that the description of the QD by the Anderson model in the presence of spin accumulation can be referred also to the mentioned Kondo alloys (conductors with magnetic impurities [5]).

II. MODEL

The considered system is schematically shown in Fig. 1. The system consists of a quantum dot coupled to a source and drain leads. The spin accumulation in the leads can be obtained by injection of nonlocal spin currents J_L, J_R [5,6,12]. The analyzed system setup is similar to the one presented in Ref. [42].

We model the QD and the Kondo alloy impurity by the Anderson Hamiltonian:

$$\begin{aligned}
 H = & \sum_{rk\sigma} \varepsilon_{rk\sigma} c_{rk\sigma}^\dagger c_{rk\sigma} + \varepsilon_0 \sum_{\sigma} d_{\sigma}^\dagger d_{\sigma} + U d_{\uparrow}^\dagger d_{\downarrow}^\dagger d_{\downarrow} \\
 & + \sum_{rk\sigma} (V_{rk\sigma} d_{\sigma}^\dagger c_{rk\sigma} + V_{rk\sigma}^* c_{rk\sigma}^\dagger d_{\sigma}) + g\mu_B B S_z, \quad (1)
 \end{aligned}$$

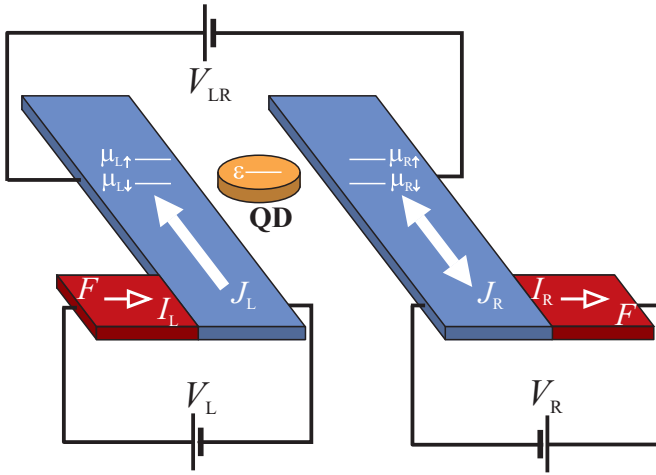


FIG. 1. The analyzed system setup. The quantum dot (QD) is coupled to source L and drain R of nonlocal lateral spin valve leads. The spin accumulation in the leads is obtained by nonlocal spin currents J_L , J_R , which results from spin polarized charge currents I_L , I_R from ferromagnetic leads F to normal leads. The direction of the spin current $J_{L(R)}$ and thus the spin accumulation $\Delta\mu_{L(R)} = \mu_{L(R)\uparrow} - \mu_{L(R)\downarrow}$ can be controlled by the direction of the charge currents $I_{L(R)}$. Arrows in the figure indicate the direction of the spin current J and the ferromagnetic leads magnetization direction.

where $c_{rk\sigma}$ ($c_{rk\sigma}^\dagger$) is the annihilation (creation) operator for electrons with momentum k and spin $\sigma = \uparrow, \downarrow$ in one of the two leads, $r = \{L, R\}$, and d_σ (d_σ^\dagger) is the annihilation (creation) operator for a σ -spin electron in the QD (impurity), $S_z = (d_\uparrow^\dagger d_\uparrow - d_\downarrow^\dagger d_\downarrow)/2$, and the last term describes the Zeeman energy of the dot (impurity), $\Delta\varepsilon = \varepsilon_\uparrow - \varepsilon_\downarrow = g\mu_B B$, $\varepsilon_\sigma = \varepsilon_0 \pm g\mu_B B/2$. We assume symmetric leads coupling and neglect the k dependence of the tunnel amplitudes, $V_{Lk} = V_{Rk} = V$. The spin accumulation in a lead r is defined by the difference between the spin-up and spin-down chemical potentials, $\Delta\mu_r \equiv \mu_{r\uparrow} - \mu_{r\downarrow}$, and is expressed in the Fermi functions:

$$f_{r\sigma}(\varepsilon) = \frac{1}{e^{(\varepsilon - \mu_{r\sigma})/k_B T} + 1}, \quad (2)$$

by the spin dependent chemical potentials $\mu_{r\sigma}$.

Following Meir and Wingreen's calculations [43–45], for the case of proportional couplings to the leads, $\Gamma_{L\sigma}(\omega) = \lambda\Gamma_{R\sigma}(\omega)$, we can express the transport current as $I = \sum_\sigma I_\sigma$, with:

$$I_\sigma = \frac{e}{\hbar} \int d\omega \frac{\Gamma_{L\sigma}(\omega)\Gamma_{R\sigma}(\omega)}{\Gamma_{L\sigma}(\omega) + \Gamma_{R\sigma}(\omega)} [f_{L\sigma}(\omega) - f_{R\sigma}(\omega)] \rho_\sigma(\omega), \quad (3)$$

where $\Gamma_{L(R)\sigma} = 2\pi|V|^2\nu_{L(R)\sigma}$; we assume a flat leads density of states $\nu_{L(R)\sigma}(\omega) = \nu$ that can be spin dependent for the ferromagnetic electrode (see Sec. IV), and $\rho_\sigma(\omega) = -(1/\pi)\text{Im}G_\sigma^{\text{ret}}(\omega)$ denotes the quantum dot density of states (DOS). Without loss of generality, we consider strong Coulomb interactions ($U \rightarrow \infty$), which simplify the retarded Green's function to:

$$G_\sigma^{\text{ret}}(\omega) = \frac{1 - \langle n_\sigma \rangle}{\omega - \varepsilon_\sigma - \Sigma_{0\sigma}(\omega) - \Sigma_{1\sigma}(\omega)}. \quad (4)$$

As we will show later, the assumption of infinite Coulomb interactions has no influence on the considered Kondo physics, despite the omission of certain details of the system. The average occupation of the QD with spin σ can be expressed as:

$$\begin{aligned} \langle n_\sigma \rangle &= -\frac{i}{2\pi} \int d\omega G_\sigma^<(\omega) \\ &= \frac{1}{2\pi} \int d\omega [-2\text{Im}G_\sigma^{\text{ret}}(\omega)] \bar{f}_\sigma(\omega), \end{aligned} \quad (5)$$

where $G^<$ is the lesser Green function, and $\bar{f}_\sigma(\omega)$ is defined as:

$$\bar{f}_\sigma(\omega) = \frac{\Gamma_{L\sigma}(\omega)f_{L\sigma}(\omega) + \Gamma_{R\sigma}(\omega)f_{R\sigma}(\omega)}{\Gamma_{L\sigma}(\omega) + \Gamma_{R\sigma}(\omega)}. \quad (6)$$

The self-energies are given by:

$$\Sigma_{0\sigma}(\omega) = \sum_{rk} \frac{|V|^2}{\omega - \varepsilon_{rk\sigma} + i0^+}, \quad (7)$$

$$\Sigma_{1\sigma}(\omega, \Delta\tilde{\varepsilon}) = \sum_{rk} \frac{|V|^2 f_{r\bar{\sigma}}(\varepsilon_{rk\bar{\sigma}})}{\omega - \sigma\Delta\tilde{\varepsilon} - \varepsilon_{rk\bar{\sigma}} + i\hbar/(2\tau_{\bar{\sigma}})}. \quad (8)$$

The above derivation was made using equations of motion method (EOM), which gives proper Kondo peaks for finite magnetic fields. The slave boson technique in the noncrossing approximation does not describe properly the influence of magnetic fields, when the mean field approximation overestimates the magnetic order, especially for large U , since it neglects quantum fluctuations [44,46,47]. The self-energy $\Sigma_{0\sigma}(\omega)$ Eq. (7) is the exact self-energy of the noninteracting case [48]. The Kondo peak for spin σ results from the self-energy $\Sigma_{1\sigma}(\omega, \Delta\tilde{\varepsilon})$, Eq. (8), due to the virtual intermediate state related to occupation of the site by the electron with opposite spin $\bar{\sigma}$. Due to the sharp Fermi surfaces at a low temperature, $\text{Re}[\Sigma_{1\sigma}(\omega, \Delta\tilde{\varepsilon})]$ grows logarithmically at $\omega = \mu_{r\sigma} \pm \Delta\tilde{\varepsilon}$ generating peaks in the DOS near those energies.

Proceeding as in Ref. [19], we extend the standard derivation [43–45] and replace in Eq. (8) $\Delta\varepsilon \equiv \varepsilon_\uparrow - \varepsilon_\downarrow \rightarrow \Delta\tilde{\varepsilon} \equiv \tilde{\varepsilon}_\uparrow - \tilde{\varepsilon}_\downarrow$, where the energy $\tilde{\varepsilon}_\sigma$ is calculated self-consistently using the relation describing the renormalized quantum dot (impurity) energy:

$$\tilde{\varepsilon}_\sigma = \varepsilon_\sigma + \text{Re}(\Sigma_{0\sigma}(\tilde{\varepsilon}_\sigma) + \Sigma_{1\sigma}(\tilde{\varepsilon}_\sigma, \Delta\tilde{\varepsilon})), \quad (9)$$

where the real part of the denominator of Eq. (4) vanishes [4]. This procedure simulates higher-order contributions and the influence of the renormalization of the dot-level $\tilde{\varepsilon}_\sigma$ on spin fluctuations. Similar to Refs. [43–45] we introduce the spin-dependent lifetime τ_σ derived by the second-order perturbation theory:

$$\begin{aligned} \frac{1}{\tau_\sigma} &= \frac{1}{\hbar} \sum_{r, r' = L, R} \Gamma_{r\sigma} \Gamma_{r'\sigma'} \Theta(\mu_{r'\sigma'} - \mu_{r\sigma} + \tilde{\varepsilon}_\sigma - \tilde{\varepsilon}_{\sigma'}) \\ &\quad \times \frac{\mu_{r'\sigma'} - \mu_{r\sigma} + \tilde{\varepsilon}_\sigma - \tilde{\varepsilon}_{\sigma'}}{(\mu_{r\sigma} - \tilde{\varepsilon}_\sigma)(\mu_{r'\sigma'} - \tilde{\varepsilon}_{\sigma'})}, \end{aligned} \quad (10)$$

which describes decoherence due to a finite bias voltage $V_{LR} = \frac{1}{2e} \sum_\sigma (\mu_{L\sigma} - \mu_{R\sigma})$, the spin accumulation, or a level splitting $\Delta\tilde{\varepsilon}$, and effectively takes into account the energy relaxation [49]. The lifetime of the intermediate state, giving

rise to $\Sigma_{1\sigma}(\omega, \Delta\tilde{\varepsilon})$, Eq. (8), becomes infinite at the zero-field and zero-temperature equilibrium, but the true peak in the DOS has an amplitude corresponding to the unitarity limit. In the presence of the bias voltage V_{LR} or a magnetic field B , the intermediate state acquires finite lifetime $\tau_{\tilde{\sigma}}$, which cuts off the logarithmic divergence of $\text{Re}[\Sigma_{1\sigma}(\omega, \Delta\tilde{\varepsilon})]$ and leads to the suppression of the peak amplitude [44].

Spin-dependent densities of states on a QD (impurity) $\rho_{\sigma}(\omega)$ are the most important qualities of the model, since they are the basis to calculate the transmission of the system in case of coupling of the QD to the leads [Eq. (3)] or the resistivity of the alloys with the magnetic impurities in the linear response [Eq. (11)]. In the first case the nonlinear response results from opening of the transport window with the electrochemical potentials in which case the corresponding range on the energy scale of the densities of states includes the Kondo peaks. These peaks give their contribution to the conductance of the system in form of distinguishable peaks in the dI/dV_{LR} signal. The linear response resistivity of the Kondo alloys can be given by the relation [40]:

$$R^{-1} = \frac{ne^2}{2m} \int \left[\sum_{\sigma} C_1 \rho_{\sigma}^{-1}(\omega) \left(-\frac{\partial f_{\sigma}(\omega)}{\partial \omega} \right) \right] d\omega, \quad (11)$$

where C_1 is a constant dependent on the concentration of the Kondo impurities. We can apply the above equation despite nonequilibrium spin accumulation Fermi level spin splitting, since for each of the spins separately the system remains in the linear response regime.

III. QUANTUM DOT COUPLED TO NORMAL ELECTRODE AND ONE WITH SPIN ACCUMULATION

First, we consider the system with a quantum dot coupled to a normal electrode and one with spin accumulation. In Fig. 2 we show the DOS for the quantum dots for various situations. As a reference system we have taken the equilibrium case of no spin accumulation [Fig. 2(a)]. In this case no spin relaxation occurs, as it can also be concluded from Eq. (10), and the densities of states for both spins are identical, with Kondo peaks centered at the energy $\omega = 0$. The presence of the spin accumulation, $\Delta\mu_R = 0.2\Gamma$, in the right lead causes a splitting of the Kondo peaks for both spins [Fig. 2(b)]. However, as shown in Refs. [37–41], the magnetic field yields the shifting of the Kondo resonances [Fig. 2(c)]. Since both the magnetic field and the spin accumulation have an impact on the position of the Kondo peaks, it is possible to counterbalance the effect of the spin accumulation by the properly tuned external magnetic field B [see Fig. 2(d)].

The Kondo peak results from successive spin-flip processes which effectively screen the local spin on the quantum dot at zero bias. In accordance with self-energy $\Sigma_{1\sigma}$ [Eq. (8)], in the electron current transmission process, which is accompanied by the spin flip process, the overall energy balance must be maintained, which means that the energy difference for the spin-flip processes in the quantum dot must correspond to the energy difference between the Fermi levels with opposite spins in the electrodes for the initial and final states:

$$\begin{aligned} \Delta\tilde{\varepsilon} &= \tilde{\varepsilon}_{\uparrow} - \tilde{\varepsilon}_{\downarrow} = g\mu_B(B + B_{ex}(p)) = \mu_{L\uparrow} - \mu_{R\downarrow} \\ &= \mu_{R\uparrow} - \mu_{L\downarrow}, \end{aligned} \quad (12)$$

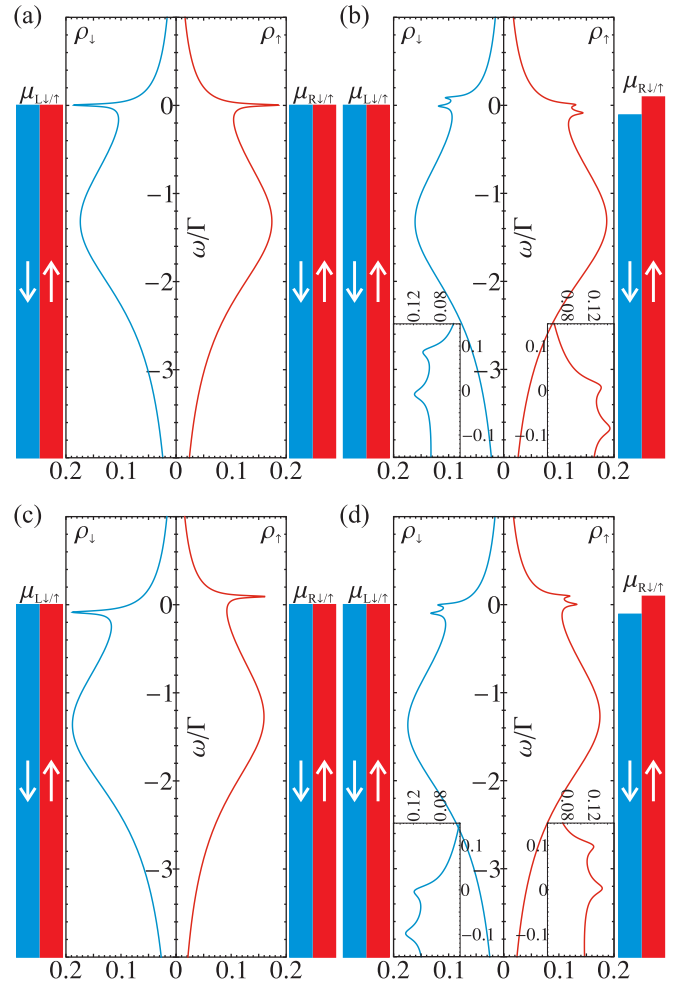


FIG. 2. Spin-dependent DOS, calculated for quantum dot coupled to: two normal leads [(a), (c)], one normal and one spin accumulated lead [(b), (d)]. (a) In the absence of Zeeman splitting $B = 0$, spin accumulation $\Delta\mu = 0$, (b) $g\mu_B B/\Gamma = 0$, $\Delta\mu_R/\Gamma = 0.2$, (c) $g\mu_B B/\Gamma = 0.1$, $\Delta\mu/\Gamma = 0$, (d) $g\mu_B B/\Gamma = 0.1$, $\Delta\mu_R/\Gamma = 0.2$. The other parameters are $V_{LR} = 0$, $k_B T/\Gamma = 0.005$, and $\varepsilon_0/\Gamma = -2$. Details of the Kondo peaks are shown in the insets. The rectangles on both left and right sides of each plot pair represent spin-dependent chemical potentials $\mu_{L\uparrow/\downarrow}$ and $\mu_{R\uparrow/\downarrow}$ for left and right lead, respectively.

where $g\mu_B B_{ex}(p) = \Delta\tilde{\varepsilon} - \Delta\varepsilon$ define the effective exchange magnetic field due to the presence of the spin polarization p in the ferromagnetic leads. Occurrence of the zero-bias anomaly requires the fulfillment of both equalities $g\mu_B(B + B_{ex}(p)) = \mu_{L\uparrow} - \mu_{R\downarrow} = \mu_{R\uparrow} - \mu_{L\downarrow}$. The split Kondo peak in the conductance is observed when only one equality from Eq. (12) is fulfilled, namely $g\mu_B(B + B_{ex}(p)) = \mu_{L\uparrow} - \mu_{R\downarrow}$ or $g\mu_B(B + B_{ex}(p)) = \mu_{R\uparrow} - \mu_{L\downarrow}$. The above result is independent of our assumption of infinite Coulomb interactions, $U \rightarrow \infty$, since the zero-bias anomaly depends solely on the magnetic field.

Observed effects in the DOS are reflected in the conductance. In Figs. 3(a)–3(d) we show the differential conductance ($G = dI/dV_{LR}$) as a function of the transport voltage V_{LR} . For normal leads one can observe well-known conductance maximum at $V_{LR} = 0$, Fig. 3(a), which is split in the

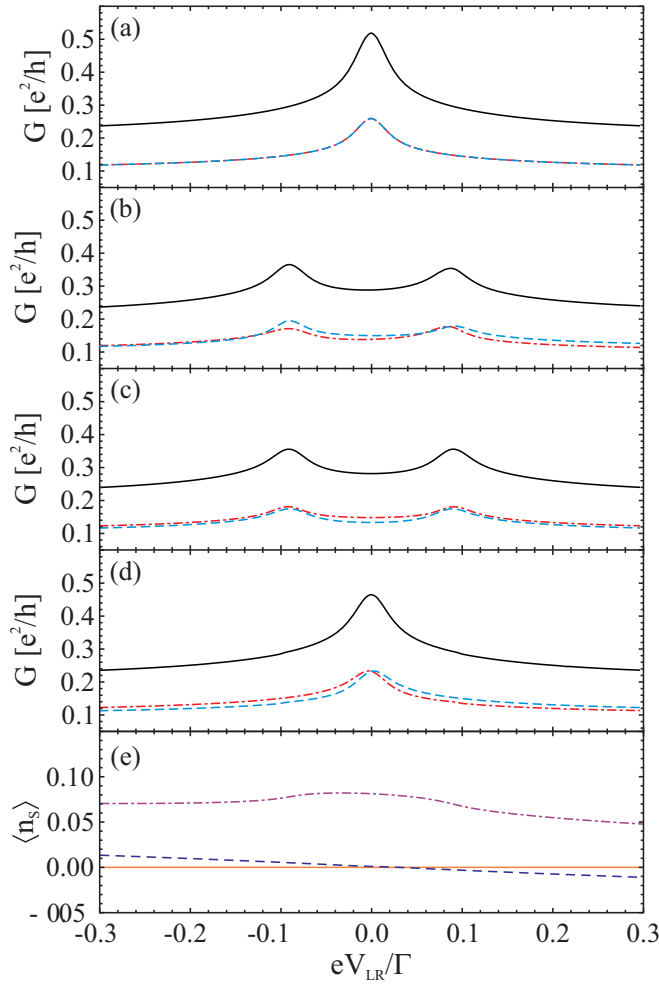


FIG. 3. (a)–(d) Total differential conductance (solid lines) and spin contributions (spin down—dashed lines, spin up—dot-dashed lines) vs the applied bias voltage eV_{LR}/Γ , for (a), (c) two normal leads and (b), (d) one normal and one spin accumulated lead. (a) Zeeman splitting $g\mu_B B/\Gamma = 0$, the spin accumulation $\Delta\mu_r/\Gamma = 0$, (b) $g\mu_B B/\Gamma = 0$, $\Delta\mu_R/\Gamma = 0.2$, $\Delta\mu_L/\Gamma = 0$, (c) $g\mu_B B/\Gamma = 0.1$, $\Delta\mu_r/\Gamma = 0$, (d) $\Delta\mu_R/\Gamma = 0.2$, $\Delta\mu_L/\Gamma = 0$, $g\mu_B B/\Gamma = 0.1$ [see Eq. (12)]. (e) The average spin occupation of the quantum dot $\langle n_s \rangle$ vs bias voltage, for two normal leads (solid line), one normal and one spin accumulated lead with $B = 0$ (dot-dashed line) and $g\mu_B B/\Gamma = 0.1$ (dashed line). The other parameters are $k_B T/\Gamma = 0.005$ and $\varepsilon_0/\Gamma = -2$.

presence of the external magnetic field [Fig. 3(c)]. Similar peak splitting can be observed for the system with a single spin accumulated lead, without magnetic field [Fig. 3(b)]. In this system zero-bias maximum can be restored by applying the appropriate magnetic field [see Eq. (12)], $g\mu_B B = \Delta\mu_R/2$ [Fig. 3(d)]. However, comparing Figs. 3(a) and 3(d), it can be seen that the zero-bias peak amplitude has decreased for the system with restored zero-bias maximum, which is a result of nonequilibrium energy balance for spin up and down between the left and right leads. The observed effect is also confirmed in Fig. 3(e), where we show the average spin occupation of the QD:

$$\langle n_s \rangle \equiv \langle n_\uparrow \rangle - \langle n_\downarrow \rangle, \quad (13)$$

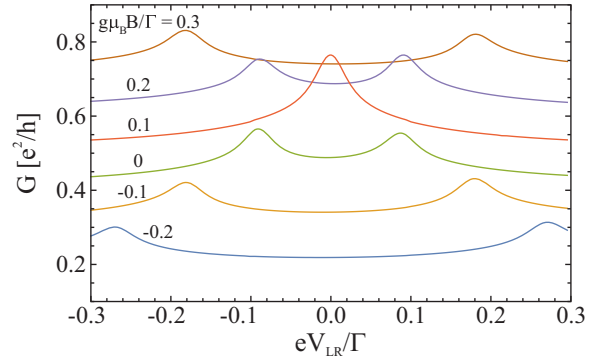


FIG. 4. Total differential conductance vs the applied bias voltage eV_{LR}/Γ for different magnetic field B , in the system with one normal and one spin accumulated lead, $\Delta\mu_L/\Gamma = 0$, $\Delta\mu_R/\Gamma = 0.2$, $k_B T/\Gamma = 0.005$, and $\varepsilon_0/\Gamma = -2$. For the magnetic field satisfying Eq. (12) one can observe nonsplit Kondo peak at zero bias.

where $\langle n_\sigma \rangle$ is defined by the Eq. (5). For QD coupled to normal leads $\langle n_s \rangle(V_{LR}) = 0$, that means full spin symmetry. As one can observe, the spin accumulation breaks the spin symmetry, and the properly tuned magnetic field does not fully recover the spin symmetry in the system. However, recovery of the zero-bias conductance peak indicates that some Kondo correlations are present in the system.

The effect of the magnetic field on the conductance is shown in Fig. 4. As one can see from the plot, the magnetic field affects the magnitude of the splitting in the conductance peaks.

IV. EFFECT OF THE LEAD SPIN POLARIZATION

As shown in Refs. [19–36], effects of magnetic field and ferromagnetic lead spin polarization on the Kondo effect in the quantum dot can compensate each other. Therefore, we

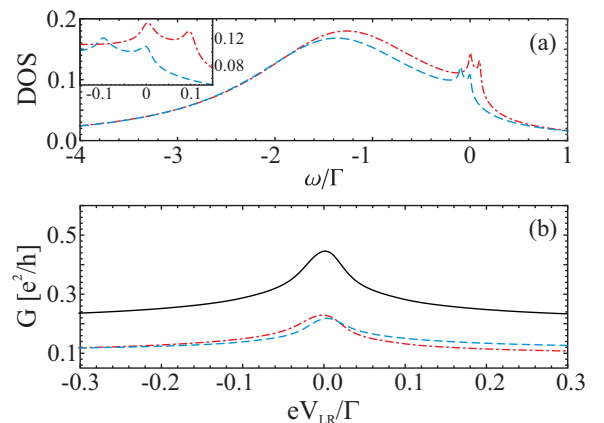


FIG. 5. (a) DOS for spin down (dashed line) and spin up (dot-dashed line) and (b) the total differential conductance (solid lines) and spin contributions (spin down—dashed lines, spin up—dot-dashed lines) vs the applied bias voltage V_{LR} , for a quantum dot coupled to ferromagnetic and spin accumulated leads, spin polarization $p_L = -0.157$, $p_R = 0$, $\Delta\mu_L/\Gamma = 0$, $\Delta\mu_R/\Gamma = 0.2$, $k_B T/\Gamma = 0.005$, and $\varepsilon_0/\Gamma = -2$. Details of the Kondo peaks are shown in the inset.

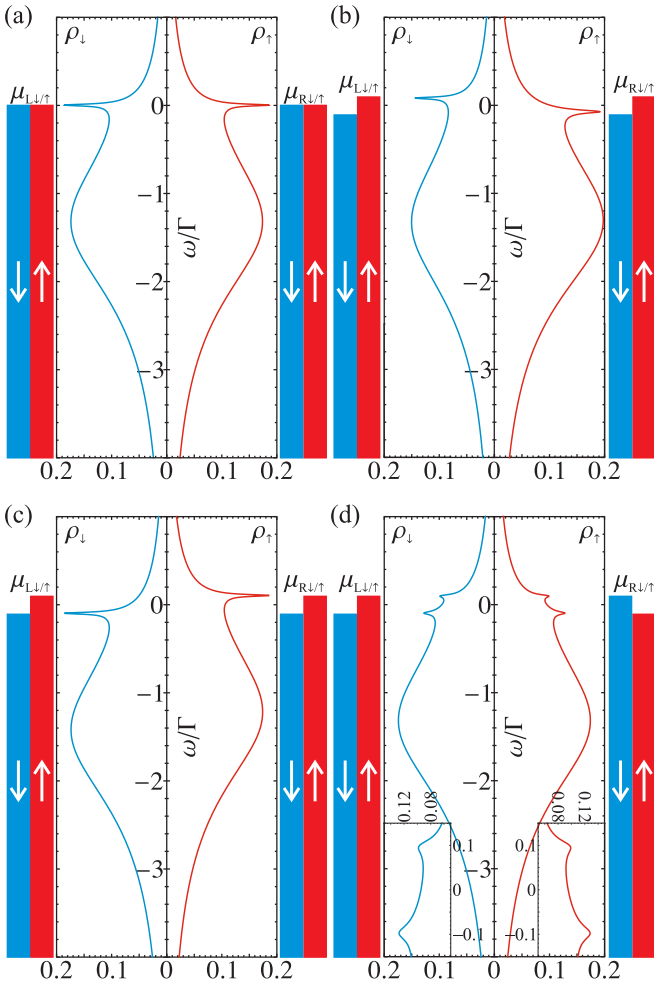


FIG. 6. Spin-dependent DOS, calculated for a quantum dot coupled to (a) two normal leads, (b)–(d) two spin accumulated leads, (b) and (c) with symmetrical spin accumulation $\Delta\mu_L = \Delta\mu_R = 0.2\Gamma$, and (d) antisymmetrical spin accumulation $\Delta\mu_L = -\Delta\mu_R = 0.2\Gamma$. (a), (b), (d) in the absence of the Zeeman splitting $B = 0$, (c) Zeeman splitting $g\mu_B B/\Gamma = 0.2$. The other parameters are $V_{LR} = 0$, $k_B T/\Gamma = 0.005$, and $\varepsilon_0/\Gamma = -2$. Details of the Kondo peaks are shown in the insets. The rectangles on both left and right sides of each plot pair represent spin-dependent chemical potentials $\mu_{L\uparrow/\downarrow}$ and $\mu_{R\uparrow/\downarrow}$ for left and right lead, respectively.

have also examined the influence of the spin polarization on the studied system. In this case we replaced the normal left electrode with the ferromagnetic one. The results are shown in Fig. 5. We define the left lead spin polarization with $p_L = (v_{L\uparrow} - v_{L\downarrow})/(v_{L\uparrow} + v_{L\downarrow})$. In the presence of the appropriate spin polarization one can also observe zero-bias conductance maximum without a spin splitting in the absence of the external magnetic field, so the Kondo effect can be restored, however the amplitude of the Kondo peak is decreased, since this system is in a nonequilibrium state for each spin component. A similar analysis was carried out in Ref. [16], however its authors considered one ferromagnetic lead with spin accumulation, which due to fast spin relaxation times in ferromagnetic materials could be hard to obtain

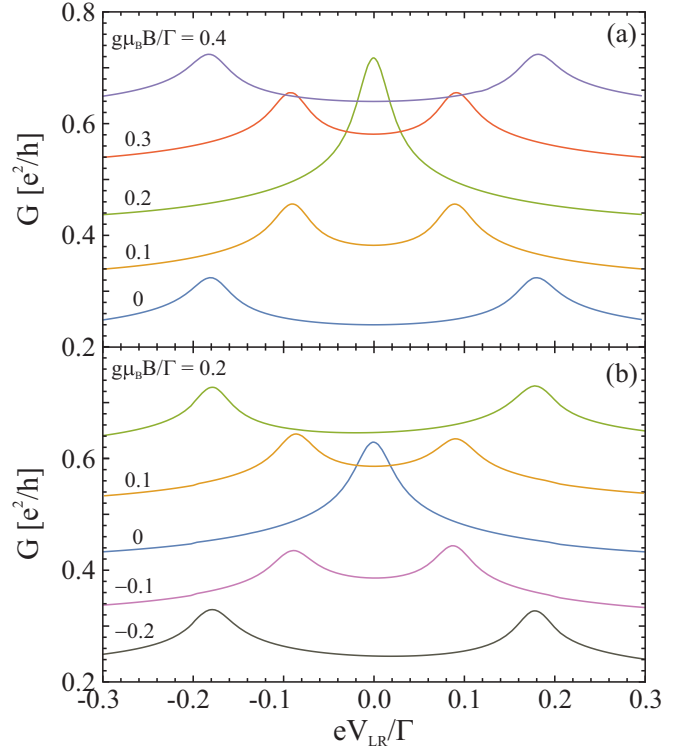


FIG. 7. Total differential conductance vs the applied bias voltage eV_{LR}/Γ for different magnetic field B in the system with two spin accumulated leads, (a) with the symmetrical spin accumulation $\Delta\mu_L = \Delta\mu_R = 0.2\Gamma$ and (b) the antisymmetrical spin accumulation $\Delta\mu_L = -\Delta\mu_R = 0.2\Gamma$; $k_B T/\Gamma = 0.005$ and $\varepsilon_0/\Gamma = -2$. For magnetic field satisfying Eq. (12) one can observe Kondo peaks.

experimentally. Our approach allows for the separation of the spin accumulation and the spin polarization to different leads.

V. QUANTUM DOT COUPLED TO TWO LEADS WITH SPIN ACCUMULATION

The second considered system is the QD coupled to two spin accumulated leads, in two possible configurations: (i) the symmetrical spin accumulation, $\Delta\mu_L = \Delta\mu_R$, and (ii) the antisymmetrical spin accumulation, $\Delta\mu_L = -\Delta\mu_R$. In the first case, the spin accumulation does not cause the splitting of the Kondo peaks; in the spin-dependent DOS for $V_{LR} = 0$, however, it causes the spin shifting of the Kondo peaks [Fig. 6(b)], opposite to the situation from Fig. 2(b). Similarly to the previously considered system, the effect of the spin accumulation can be counterbalanced by the magnetic field, Fig. 6(c), according to Eq. (12). The conductance vs bias voltage for the different magnetic field values is shown in Fig. 7(a). Similarly to the previous studied system, Fig. 4, the magnetic field affects the size of the zero bias anomaly splitting. In Fig. 8(a), we show the differential conductance for symmetrical spin accumulation $\Delta\mu_L = \Delta\mu_R = 0.2\Gamma$. As one can see from Fig. 8(b) the properly tuned magnetic field (we set $g\mu_B B = \Delta\mu_L = \Delta\mu_R$ to restore zero-bias peak) restores the zero-bias maximum. However, in this system setup, the

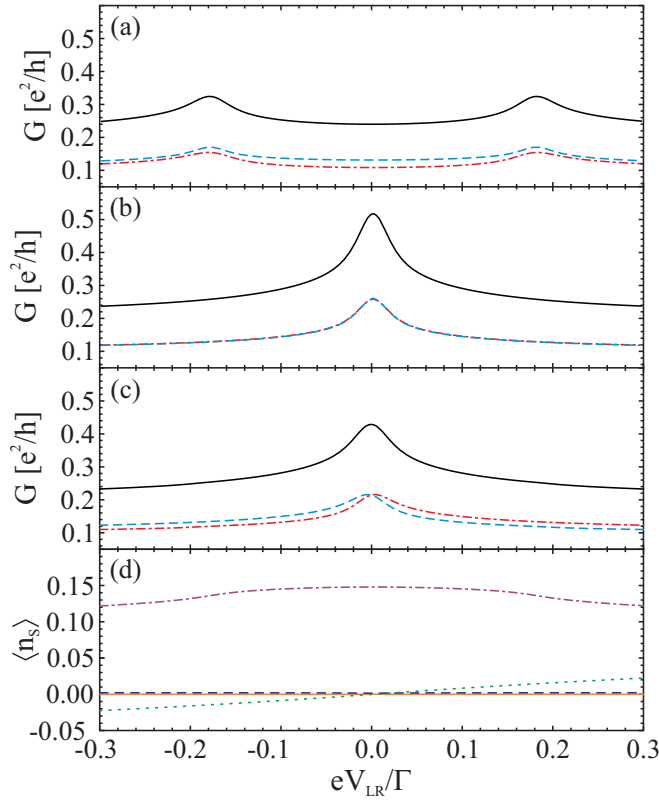


FIG. 8. Total differential conductance (solid lines) and spin contributions (spin down—dashed lines, spin up—dot-dashed lines) vs the applied bias voltage V_{LR} , for a quantum dot coupled to two spin accumulated leads: (a), (b) with the symmetrical spin accumulation $\Delta\mu_L = \Delta\mu_R = 0.2\Gamma$ and (c) the antisymmetrical spin accumulation $\Delta\mu_L = -\Delta\mu_R = 0.2\Gamma$. Zeeman splitting [(a), (c)] $B = 0$, (b) $g\mu_B B/\Gamma = 0.2$ [see Eq. (12)]. (d) The average spin occupation of the quantum dot $\langle n_s \rangle$ vs bias voltage, for two normal leads (solid line), for two symmetrically spin accumulated leads, $\Delta\mu_L = \Delta\mu_R$, with $B = 0$ (dot-dashed line) and $g\mu_B B/\Gamma = 0.2$ (dashed line), and for two antisymmetrically spin accumulated leads, $\Delta\mu_L = -\Delta\mu_R$, with $B = 0$ (dotted line). The other parameters are $k_B T/\Gamma = 0.005$ and $\varepsilon_0/\Gamma = -2$.

peak amplitude remained the same as in Fig. 3(a). This is a result of conserved energy balance for spin up and down between left and right electrode. Therefore, for each spin component separately the system remains in equilibrium. Also in this case the observed effect is confirmed by the average spin occupation of the QD $\langle n_s \rangle$ [see Fig. 8(e)]. The properly tuned magnetic field, $g\mu_B B = \Delta\mu_L = \Delta\mu_R$, fully recovers the SU(2) symmetry, so the strong coupling limit of the Kondo effect is possible in the system.

In the second considered system, due to the effect of the antisymmetrical spin accumulation, $\Delta\mu_L = -\Delta\mu_R$, one can observe the zero-bias conductance maximum [Fig. 8(c)]. In the spin-dependent DOS the Kondo peaks are symmetrically split for both spins, and their position corresponds to leads chemical potentials [Fig. 6(d)]. Unlike the symmetrical case, in this system, the spin accumulation affects the amplitude of the zero-bias anomaly; see Fig. 9(a). As the spin accumulation increases, for the antisymmetric system, the zero bias anomaly peak height decreases, while for the symmetrical

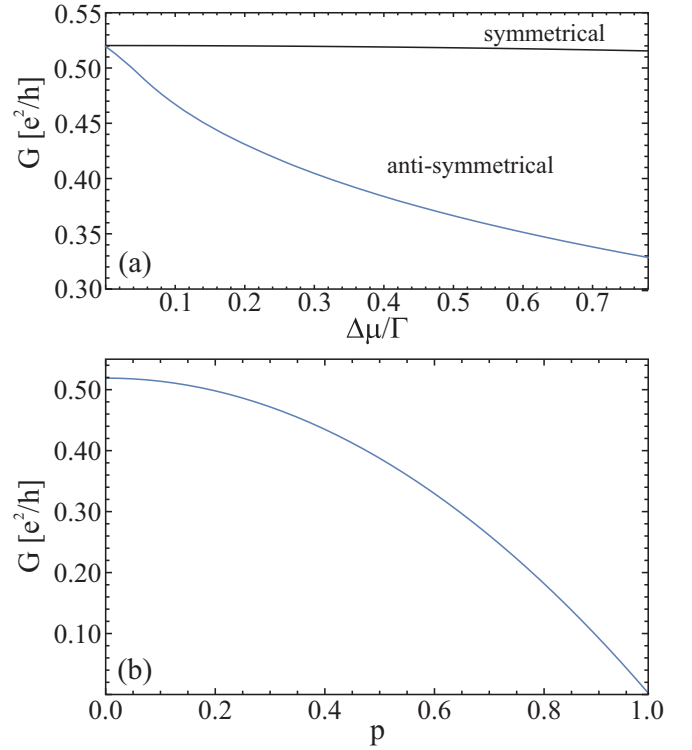


FIG. 9. Total differential conductance G for $eV_{LR}/\Gamma = 0$ vs (a) spin accumulation $\Delta\mu_r$, for the symmetrical $\Delta\mu_L = \Delta\mu_R = \Delta\mu$ and the antisymmetrical $\Delta\mu_L = -\Delta\mu_R = \Delta\mu$ system, (b) spin polarization p for system with ferromagnetic leads in antiparallel configuration $p_L = -p_R = p$. Magnetic field for the symmetrical system $g\mu_B B = \Delta\mu_r$ and for the antisymmetrical system with ferromagnetic leads $B = 0$. The other parameters are $k_B T/\Gamma = 0.005$ and $\varepsilon_0/\Gamma = -2$.

system the peak height is constant (in this case $\tau_\sigma^{-1} \rightarrow 0$). In comparison to the system with two ferromagnetic leads without spin accumulation in the antiparallel configuration $p_L = -p_R = p$ [19], the height of the zero bias anomaly peak decreases as a function of $1 - p^2$, which is shown in Fig. 9(b). Same as before, the zero-bias conductance peak indicates that some Kondo correlations are present in the system.

For the above-mentioned results the relevant parameter is the spin relaxation time τ_{sf} , which should be longer than $\tau_K = \hbar/(k_B T_K)$. For example, as Ref. [7] shows, the spin-flip time for Cu wire, $\tau_{sf} = 42$ ps at 4.2 K, and 11 ps at room temperature. The Kondo temperature for Cu(Fe) wire $T_K = 30$ K, as shown in Ref. [12], indicating relaxation $\tau_K \simeq 10$ ps, which is sufficient for the experimental observation of the discussed effect.

VI. SPIN CURRENT IN KONDO ALLOYS

The Anderson model can also be used for the description of the transport properties of the Kondo alloys. In the experiments [5,12], spin current injection into the Kondo alloy partially cancels the Kondo effect observed as a logarithmic increase of resistance with lowering of the temperature. Also the resistivity of the system is dependent on the current direction. The authors of these works concluded that the

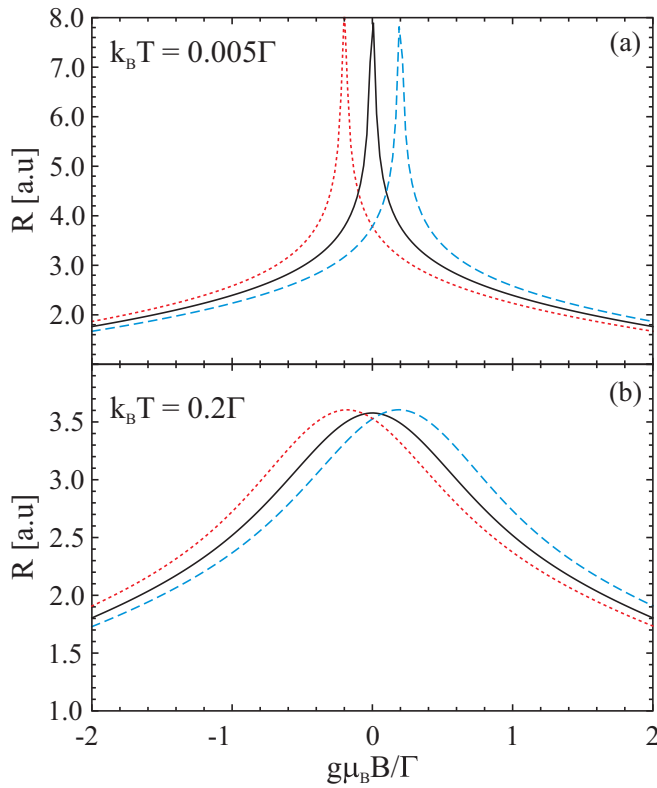


FIG. 10. Resistance R vs magnetic field B calculated for the Kondo impurity in alloy without spin accumulation (solid lines) and spin accumulated alloy: $\Delta\mu = 0.2\Gamma$ —dashed lines and $\Delta\mu = -0.2\Gamma$ —dotted lines, (a) $k_B T/\Gamma = 0.005$ (b) $k_B T/\Gamma = 0.2$; $\varepsilon_0/\Gamma = -2$.

presence of the local spin accumulation induced by the spin current was the reason for these effects. We show here in detail how the alloy magnetic impurities, modeled as Anderson QDs in the presence of spin accumulation, can explain the mentioned phenomena. In this situation however, the increase in resistivity instead of conductance increase is observed in the linear response regime; the Kondo state plays the role of the scatterer in the electron movement through the metal. The Kondo peak structure appearing in the calculated resistivity signal (Fig. 10) according to Eq. (11) is analogous to the conductance peak appearing for quantum dots. Both spins' contribution for the total resistivity can be calculated separately, so if the spin accumulation occurs in the system, the peak in resistivity for an unbiased system moves out from the zero-bias regime, as can be seen in Fig. 10, where the peak position change is probed by plotting the resistance as a function of the external magnetic field. The peak position depends on the value of the spin accumulation due to a dependence of the Fermi function on the spin accumulation as in Eq. (11).

Similarly, we can analyze the resistance vs spin accumulation dependence; see Fig. 11. In the absence of the external magnetic field, increasing spin accumulation lowers the resistance value. The magnetic field causes the shift of the resistance peak, similarly to the previous considered case. The correctness of our model is confirmed by the experimentally observed dependence of the spin signal ΔR_S versus current I in Ref. [12], which is the measure of the spin accumulation

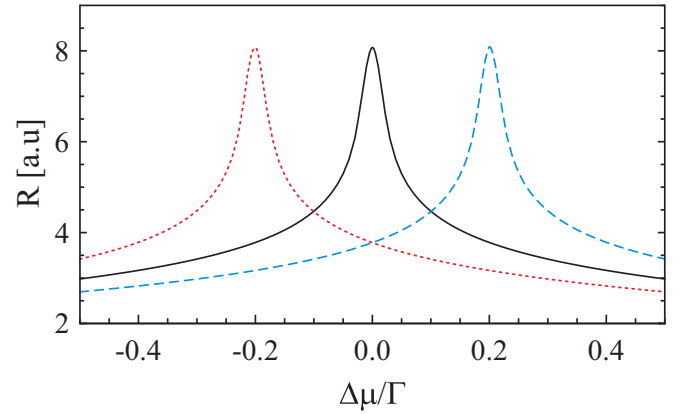


FIG. 11. Resistance R vs spin accumulation $\Delta\mu$ calculated for the Kondo impurity in alloy with spin accumulation $\Delta\mu$, for magnetic field: $B = 0$ —solid line, $g\mu_B B/\Gamma = 0.2$ —dashed line and $g\mu_B B/\Gamma = -0.2$ —dotted line; $k_B T/\Gamma = 0.005$; $\varepsilon_0/\Gamma = -2$.

in the nonlocal lateral spin valve (LSV) geometry. In Fig. 12 we compare our results with those obtained by K. Hamaya *et al.* [12]. In the experiment authors measure the spin valve signal ΔR_S for a $\text{Co}_2\text{FeSi-Cu-Co}_2\text{FeSi}$ LSV, which depends on the change in $\Delta\mu$ in the host Cu.

VII. CONCLUSION

We studied the influence of the spin accumulation in the leads on conductance in Kondo systems such as a quantum dot coupled to (i) one normal and one spin accumulated lead and (ii) two spin accumulated leads. We developed the theoretical model of the systems and analyzed its properties, which made it possible to study the mutual influence of various factors such as spin accumulation, external magnetic field, and spin polarization in the case of using ferromagnetic electrodes on the spin-dependent density of states, and on the electrical conductivity and resistance for the quantum dot and magnetic

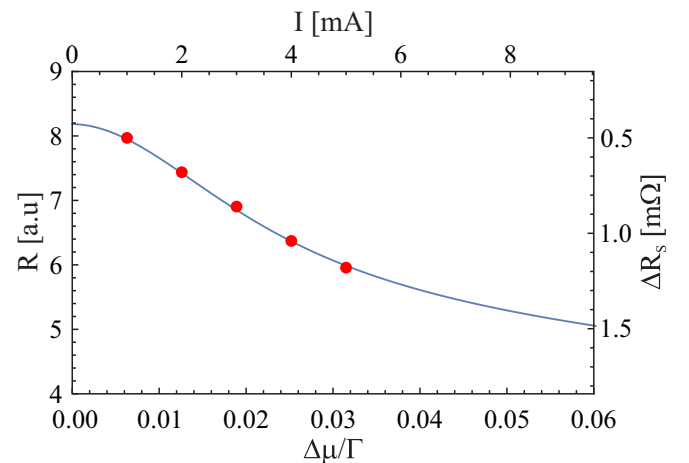


FIG. 12. Resistance R vs spin accumulation $\Delta\mu$ calculated for the Kondo impurity in alloy with spin accumulation $\Delta\mu$ (left and down axes), and ΔR_S vs current I generating the spin accumulation (up and right axes) in the LSV (data from Ref. [12]). The other parameters are $B = 0$, $k_B T/\Gamma = 0.005$, and $\varepsilon_0/\Gamma = -2$.

impurity. It has been shown that the presence of these factors by breaking the spin symmetry leads to the suspension of the Kondo effect. However, surprisingly, the effects derived from the above-mentioned factors can, for appropriately selected parameter values, compensate each other, which may lead to the restoration of the Kondo effect in the analyzed systems.

ACKNOWLEDGMENT

We would like to thank J. Barnaś, J. König, and T. Taniyama for helpful discussions. Authors received support from National Science Centre, Poland, Grants No. 2015/17/B/ST3/02799, No. 2020/36/C/ST3/00539, and No. 2017/27/B/ST3/00621.

-
- [1] J. Kondo, Resistance minimum in dilute magnetic alloys, *Prog. Theor. Phys.* **32**, 37 (1964).
- [2] P. Nozières and A. Blandin, Kondo effect in real metals, *J. Phys.* **41**, 193 (1980).
- [3] M. Pustilnik and L. I. Glazman, Kondo Effect in Real Quantum Dots, *Phys. Rev. Lett.* **87**, 216601 (2001).
- [4] A. C. Hewson, *The Kondo Problem to Heavy Fermions* (Cambridge University Press, Cambridge, 1993).
- [5] T. Taniyama, N. Fujiwara, Y. Kitamoto, and Y. Yamazaki, Asymmetric Transport Due to Spin Injection Into a Kondo Alloy, *Phys. Rev. Lett.* **90**, 016601 (2003).
- [6] T. Kobayashi, S. Tsuruta, S. Sasaki, T. Fujisawa, Y. Tokura, and T. Akazaki, Kondo Effect in a Semiconductor Quantum Dot with a Spin-Accumulated Lead, *Phys. Rev. Lett.* **104**, 036804 (2010).
- [7] F. J. Jedema, A. T. Filip, and B. J. van Wees, Electrical spin injection and accumulation at room temperature in an all-metal mesoscopic spin valve, *Nature (London)* **410**, 345 (2001).
- [8] F. J. Jedema, M. S. Nijboer, A. T. Filip, and B. J. van Wees, Spin injection and spin accumulation in all-metal mesoscopic spin valves, *Phys. Rev. B* **67**, 085319 (2003).
- [9] E. Villamor, M. Isasa, L. E. Hueso, and F. Casanova, Temperature dependence of spin polarization in ferromagnetic metals using lateral spin valves, *Phys. Rev. B* **88**, 184411 (2013).
- [10] L. O'Brien, M. J. Erickson, D. Spivak, H. Ambaye, R. J. Goyette, V. Lauter, P. A. Crowell, and C. Leighton, Kondo physics in non-local metallic spin transport devices, *Nat. Commun.* **5**, 3927 (2014).
- [11] J. T. Batley, M. C. Rosamond, M. Ali, E. H. Linfield, G. Burnell, and B. J. Hickey, Spin relaxation through Kondo scattering in cu/py lateral spin valves, *Phys. Rev. B* **92**, 220420(R) (2015).
- [12] K. Hamaya, T. Kurokawa, S. Oki, S. Yamada, T. Kanashima, and T. Taniyama, Direct evidence for suppression of the Kondo effect due to pure spin current, *Phys. Rev. B* **94**, 140401(R) (2016).
- [13] L. O'Brien, D. Spivak, J. S. Jeong, K. A. Mkhoyan, P. A. Crowell, and C. Leighton, Interdiffusion-controlled Kondo suppression of injection efficiency in metallic nonlocal spin valves, *Phys. Rev. B* **93**, 014413 (2016).
- [14] J. D. Watts, J. S. Jeong, L. O'Brien, K. A. Mkhoyan, P. A. Crowell, and C. Leighton, Room temperature spin Kondo effect and intermixing in co/cu non-local spin valves, *Appl. Phys. Lett.* **110**, 222407 (2017).
- [15] Y. Qi, J.-X. Zhu, S. Zhang, and C. S. Ting, Kondo resonance in the presence of spin-polarized currents, *Phys. Rev. B* **78**, 045305 (2008).
- [16] J. S. Lim, R. López, L. Limot, and P. Simon, Nonequilibrium spin-current detection with a single Kondo impurity, *Phys. Rev. B* **88**, 165403 (2013).
- [17] S. Sahoo, A. Crépieux, and M. Lavagna, Out-of-equilibrium Kondo effect in a quantum dot: Interplay of magnetic field and spin accumulation, *Europhys. Lett.* **116**, 57005 (2016).
- [18] T.-F. Fang, A.-M. Guo, and Q.-F. Sun, Nonequilibrium Kondo effect by the equilibrium numerical renormalization group method: The hybrid anderson model subject to a finite spin bias, *Phys. Rev. B* **97**, 235115 (2018).
- [19] J. Martinek, Y. Utsumi, H. Imamura, J. Barnaś, S. Maekawa, J. König, and G. Schön, Kondo Effect in Quantum Dots Coupled to Ferromagnetic Leads, *Phys. Rev. Lett.* **91**, 127203 (2003).
- [20] J. Martinek, M. Sindel, L. Borda, J. Barnaś, J. König, G. Schön, and J. von Delft, Kondo Effect in the Presence of Itinerant-Electron Ferromagnetism Studied with the Numerical Renormalization Group Method, *Phys. Rev. Lett.* **91**, 247202 (2003).
- [21] M. Braun, J. König, and J. Martinek, Theory of transport through quantum-dot spin valves in the weak-coupling regime, *Phys. Rev. B* **70**, 195345 (2004).
- [22] A. N. Pasupathy, R. C. Bialczak, J. Martinek, J. E. Grose, L. A. K. Donev, P. L. McEuen, and D. C. Ralph, The kondo effect in the presence of ferromagnetism, *Science* **306**, 86 (2004).
- [23] Y. Utsumi, J. Martinek, G. Schön, H. Imamura, and S. Maekawa, Nonequilibrium Kondo effect in a quantum dot coupled to ferromagnetic leads, *Phys. Rev. B* **71**, 245116 (2005).
- [24] J. Martinek, M. Sindel, L. Borda, J. Barnaś, R. Bulla, J. König, G. Schön, S. Maekawa, and J. von Delft, Gate-controlled spin splitting in quantum dots with ferromagnetic leads in the Kondo regime, *Phys. Rev. B* **72**, 121302(R) (2005).
- [25] I. Weymann, J. Barnaś, J. König, J. Martinek, and G. Schön, Zero-bias anomaly in cotunneling transport through quantum-dot spin valves, *Phys. Rev. B* **72**, 113301 (2005).
- [26] J. Martinek, L. Borda, Y. Utsumi, J. König, J. von Delft, D. Ralph, G. Schön, and S. Maekawa, Kondo effect in single-molecule spintronic devices, *J. Magn. Magn. Mater.* **310**, e343 (2007).
- [27] M. Sindel, L. Borda, J. Martinek, R. Bulla, J. König, G. Schön, S. Maekawa, and J. von Delft, Kondo quantum dot coupled to ferromagnetic leads: Numerical renormalization group study, *Phys. Rev. B* **76**, 045321 (2007).
- [28] K. Hamaya, M. Kitabatake, K. Shibata, M. Jung, M. Kawamura, K. Hirakawa, T. Machida, T. Taniyama, S. Ishida, and Y. Arakawa, Kondo effect in a semiconductor quantum dot coupled to ferromagnetic electrodes, *Appl. Phys. Lett.* **91**, 232105 (2007).
- [29] J. R. Hauptmann, J. Paaske, and P. E. Lindelof, Electric-field-controlled spin reversal in a quantum dot with ferromagnetic contacts, *Nat. Phys.* **4**, 373 (2008).
- [30] H. Yang, S.-H. Yang, G. Ilnicki, J. Martinek, and S. S. P. Parkin, Coexistence of the Kondo effect and a ferromagnetic phase in magnetic tunnel junctions, *Phys. Rev. B* **83**, 174437 (2011).

- [31] M. Gaass, A. K. Hüttel, K. Kang, I. Weymann, J. von Delft, and C. Strunk, Universality of the Kondo Effect in Quantum Dots with Ferromagnetic Leads, *Phys. Rev. Lett.* **107**, 176808 (2011).
- [32] R. Žitko, J. S. Lim, R. López, J. Martinek, and P. Simon, Tunable Kondo Effect in a Double Quantum Dot Coupled to Ferromagnetic Contacts, *Phys. Rev. Lett.* **108**, 166605 (2012).
- [33] A. Dirnauichner, M. Grifoni, A. Prüfling, D. Steininger, A. K. Hüttel, and C. Strunk, Transport across a carbon nanotube quantum dot contacted with ferromagnetic leads: Experiment and nonperturbative modeling, *Phys. Rev. B* **91**, 195402 (2015).
- [34] D.-J. Choi, S. Guissart, M. Ormaza, N. Bachelier, O. Bengone, P. Simon, and L. Limot, Kondo resonance of a co atom exchange coupled to a ferromagnetic tip, *Nano Lett.* **16**, 6298 (2016).
- [35] A. D. Crisan, S. Datta, J. J. Viennot, M. R. Delbecq, A. Cottet, and T. Kontos, Harnessing spin precession with dissipation, *Nat. Commun.* **7**, 10451 (2016).
- [36] G. D. Scott and T.-C. Hu, Gate-controlled kondo effect in a single-molecule transistor with elliptical ferromagnetic leads, *Phys. Rev. B* **96**, 144416 (2017).
- [37] D. Goldhaber-Gordon, H. Shtrikman, D. Mahalu, D. Abusch-Magder, U. Meirav, and M. A. Kastner, Kondo effect in a single-electron transistor, *Nature (London)* **391**, 156 (1998).
- [38] S. M. Cronenwett, T. H. Oosterkamp, and L. P. Kouwenhoven, A tunable kondo effect in quantum dots, *Science* **281**, 540 (1998).
- [39] J. E. Moore and X.-G. Wen, Anomalous Magnetic Splitting of the Kondo Resonance, *Phys. Rev. Lett.* **85**, 1722 (2000).
- [40] T. A. Costi, Kondo Effect in a Magnetic Field and the Magnetoresistivity of Kondo Alloys, *Phys. Rev. Lett.* **85**, 1504 (2000).
- [41] T. A. Costi, Magnetotransport through a strongly interacting quantum dot, *Phys. Rev. B* **64**, 241310(R) (2001).
- [42] S. F. Svensson, E. A. Hoffmann, N. Nakpathomkun, P. M. Wu, H. Q. Xu, H. A. Nilsson, D. Sánchez, V. Kashcheyevs, and H. Linke, Nonlinear thermovoltage and thermocurrent in quantum dots, *New J. Phys.* **15**, 105011 (2013).
- [43] Y. Meir and N. S. Wingreen, Landauer Formula for the Current through an Interacting Electron Region, *Phys. Rev. Lett.* **68**, 2512 (1992).
- [44] Y. Meir, N. S. Wingreen, and P. A. Lee, Low-Temperature Transport through a Quantum Dot: The Anderson Model Out of Equilibrium, *Phys. Rev. Lett.* **70**, 2601 (1993).
- [45] N. S. Wingreen and Y. Meir, Anderson model out of equilibrium: Noncrossing-approximation approach to transport through a quantum dot, *Phys. Rev. B* **49**, 11040 (1994).
- [46] V. Dorin and P. Schlottmann, Slave-boson mean-field theory of the anderson lattice with finite u and orbital degeneracy, *Phys. Rev. B* **47**, 5095 (1993).
- [47] V. Dorin and P. Schlottmann, Ferromagnetic instability in a mean-field slave-boson approach for the anderson lattice, *J. Appl. Phys.* **73**, 5400 (1993).
- [48] H. Haug and A.-P. Jauho, *Quantum Kinetics in Transport and Optics of Semiconductors* (Springer, Berlin, Heidelberg, 2008).
- [49] A. Kaminski and L. I. Glazman, Electron Energy Relaxation in the Presence of Magnetic Impurities, *Phys. Rev. Lett.* **86**, 2400 (2001).